Low-latitude "dusty events" vs. high-latitude "icy Heinrich events"

Elsa Jullien, Francis Grousset, Bruno Malaizé, Josette Duprat, Maria Fernanda Sanchez-Goni, Frédérique Eynaud, Karine Charlier, Ralph Schneider, Aloys Bory, Viviane Bout-roumazeilles, et al.

Low-latitude "dusty events" vs. high-latitude "icy Heinrich events"

Elsa Jullien [a,*], Francis Grousset [a], Bruno Malaizé [a], Josette Duprat [a], Maria Fernanda Sanchez-Goni [a], Frédérique Eynaud [a], Karine Charlier [a], Ralph Schneider [b], Aloys Bory [c], Viviane Bout [c], Jose Abel Flores [d]

[a] EPOC, UMR 5805, Université Bordeaux I, 33405 Talence, France

[b] Institut für Geowissenschaften, Christian-Albrechts-Universitaet, 10/24118 Kiel, Germany

[c] PBDS, UMR 8110 CNRS, Université de Lille 1, 59655 Villeneuve d'Ascq, France

[d] Departamento de Geología, Universidad de Salamanca, 37008, Salamanca, Spain

*Corresponding author. Fax: +33 556 840 848. E-mail address: e.jullien@epoc.u-bordeaux1.fr (E. Jullien).

Abstract

It has been proposed that tropical events could have participated in the triggering of the classic, high-latitude, iceberg-discharge Heinrich events (HE). We explore low-latitude Heinrich events equivalents at high resolution, in a piston core recovered from the tropical north-western African margin. They are characterized by an increase of total dust, lacustrine diatoms and fibrous lacustrine clay minerals. Thus, low-latitude events clearly reflect severe aridity events that occurred over Africa at the Saharan latitudes, probably induced by southward shifts of the Inter Tropical Convergence Zone. At a first approximation, it seems that there is more likely synchronicity between the high-latitude Heinrich Events (HEs) and low-latitude events (LLE), rather than asynchronous behaviours.

Keywords: Pleistocene; Low-latitudes; Heinrich events; Dust; Ti/Al; Clays

Introduction

It is now well known that, during the last glacial period, abrupt massive discharges of Laurentide-derived icebergs – the so-called Heinrich Events (HEs) – invaded the northern Atlantic ocean, inducing ice-rafted detritus (IRD) accumulations on the oceanic bottom every 5–10 kyr (Heinrich, 1988). Since that pioneering article, many hypotheses have been proposed to explain the origin of these events. One of them – the "internal forcing hypothesis" (McAyeal, 1993) requiring cyclic meltings of the basal ice sheet that would have triggered

Laurentide surges – is largely accepted by most paleoclimatologists, although some aspects of the theory are still unsatisfactory. In parallel, similar events have been observed worldwide: these could be a remote response to the HEs, the signal being transported either through hydrological means and/or through atmospheric teleconnections (Broecker, 2003), but such a link has not been demonstrated yet. An alternate scenario could be provided by considering the tropical ocean–atmosphere system as a potential trigger for the initiation of HEs (Cane and Clement, 1999). In order to explore this possible low-latitude forcing, we have studied a sediment core from the eastern tropical North Atlantic Ocean, focusing on the identification of possible low-latitude abrupt events imprints. Here, we present the lithic characteristics of these low-latitude events (LLE), that include anomalies in dust abundance, mean grain-size, mineralogy, elemental and isotopic compositions. Significant changes in these parameters should reflect simultaneous changes in dryness/humidity over the nearby continent. Considering their timing, we may try to assess whether the observed low-latitude dusty events are synchronous with, or whether or not they lead/ lag the typical high-latitude icy HEs.

Core selection and methods

The present-day climatic conditions over NW Africa are mostly controlled by latitudinal shifts of the Inter Tropical Convergence Zone (ITCZ). This latitudinal boundary roughly separates northern dry air conditions and equatorial monsoonal wet regimes. In summers, the ITCZ moves up to its northernmost position (20°N in August) (Fig. 1). In the northern Sahara regions, dry climatic conditions prevail, fostering dust deflation and transport. Dust is then transported across the Saharan margin by northeasterly to easterly winds. The mean position of the dust plume over the tropical Atlantic ocean lies between 15° and 25°N along an E–W axis. In winter, the ITCZ migrates, as far south as 5°N latitude, drastically expanding the continental area affected by dry conditions and strong winds. The Harmattan winds dominate in the lower part of the atmosphere (less than 1 km), whereas at higher altitudes (1– 3 km), easterly Saharan Air Layer (SAL) winds transport and unload Saharan dust over the North Atlantic ocean, between 5° and 15°N. North–south movements of ITCZ would respond to changes in interhemispheric temperature gradient, inducing southward displacements during colder periods (Broccoli et al., 2006). Considering this context, we have recovered a core located below this dust plume (Fig. 1), anticipating a relevant record of the Saharan dust variability over the last glacial period and including any potential high-frequency climatic change.

The IMAGES Calypso-core MD03-2705 was recovered on a seamount, off the Mauritanian coast (18°05N; 21°09W; 3085 m water depth) (Fig. 1). This seamount is located on a submarine ridge connecting the Cape Verde Archipelago to the African margin. The seamount culminates at about 300 m above the submarine ridge. Accordingly, the site is not likely to have received sediment by bottom current advection (Moyes et al., 1976). The area was also not supplied by riverine outputs (Kolla et al., 1979). We do not observe any mass flow deposits, but do see rare traces of burrowing. Core MD03-2705 is clearly located within the modern summer African dust plume, but at the northern boundary of the winter dust plume (Husar et al., 1997).

Considering this particular environmental setting, it can be assumed that, over the last climatic cycle, this continuous, sandy-ooze marine record was solely built up by two main components: a biogenic, calcareous fraction and a terrigenous, detrital aeolian fraction:

- the biogenic particles derived from the surface water masses were mainly composed of foraminifera and coccoliths. The biogenic opal component (diatoms) is considered to be negligible (<5% (deMenocal et al., 2000)).
- the terrigenous fraction is mostly made of Sahara/Sahel derived aerosols. This dust fraction is a mixture of clay minerals and fine silt-sized quartz brought by the winds, along with freshwater diatoms and phytoliths. We characterized the dust fraction in core MD03-2705, using several techniques: (i) the percentage of carbonate was obtained by the gasometric method. As the biogenic-opal component is negligible (deMenocal et al., 2000), we consider that particles which are not biogenic are dust, whatever their size. Indeed, the % dust=100%−carbonate %; (ii) grain-size analyses were performed on the carbonate-free fraction using the Malvern laser-beam grain-size analyzer (Mie, 1908); (iii) the clay mineral composition was measured using X-ray diffractometry (Holtzapffel, 1985); (iv) the Sr and Nd isotopic compositions were measured on the fine (<40 μm), carbonate-free fraction of the sediments, using the same procedure as that previously used in this region (Grousset et al., 1998); (v) finally, the composition of minor/trace elements was measured on the bulk sediments (Jansen et al., 1998), using the Bremen XRF-Cortex facility, focusing in particular on the Ti/Al ratio, as it is considered to be a good proxy of wind intensity (Boyle, 1983).

Results

In this paper, we focused on the seven upper meters of the 37-m-long core MD03-2705 in order to specifically bracket the last glacial period, which should contain, if present, the abrupt LLEs. The age model is based on a comparison of the $\delta^{18}O$/ $\delta^{13}C$ record obtained on the benthic foraminifera Planulina wuellerstorfi (Fig. 2; Table 1), with the SPECMAP record (Martinson et al., 1987) and the $\delta^{18}O$ record obtained by deMenocal et al., 2000 on the neighbouring core ODP-658C (Fig. 1). To better constrain this age model, eight AMS-14C ages were obtained on the planktic foraminifera Globigerina bulloides (N150 μm), over the last 30 kyr. Due to the possible influence of upwelling water filaments in the area, we corrected 14C dates using a conservative reservoir age of 500 yr (deMenocal et al., 2000). Afterwards, these radiocarbon ages were calibrated to calendar ages (Bard, 1988; Stuiver et al., 2005). Three other independent time horizons were provided by major changes in foraminifera assemblages: an abrupt increase of Globorotalia menardii defining the Holocene inception, an abrupt decrease in Globorotalia inflata at the beginning of the Last Glacial Maximum (LGM) and its abrupt increase at the base of the Bolling-Alleröd. This age model is consistent with a record obtained in the neighbouring core CD53-30 (Matthewson et al., 1995) (Fig. 1). The age of the core top is around 4.3 kyrs (cal. age), indicating that the upper Holocene sediments were not recovered during the coring process. Accumulation rates were not calculated, as the upper meters of Calypso cores are often affected by stretching effects due to cable rebound causing upward piston acceleration (Skinner and McCave, 2003). Due to its low accumulation rate, core MD03-2705 cannot record high-frequency (sub-centennial scales) climatic changes, but it allows us to document large amplitude changes that characterized the last 75 ka, i.e. glacial– interglacial changes as well as abrupt millennial-scale events, if any.

During interglacial periods (stages 1 and 5), dust contents are low (≈33%), fine particles dominate (only 18% >40 μm) and the sediment color is relatively light (low Ti and Fe abundances; high reflectance), indicating basically a dominant biogenic ($CaCO_3$) supply. Important changes in the terrigenous fraction characterize both the last glacial period and the Younger Dryas episode: compared to interglacials, the dust abundance increases from ≈30% to ≈55% (Fig. 2), the particle mean size increases (the N40 μm fraction representing up to ≈30%) as well as their density (twice as much as Ti, Fe and Si). As previously observed in many other cores, MIS 3 was characterized by “warmer” conditions compared with MIS 2 or 4 (Imbrie et al., 1984).

Within the last glacial period, five abrupt events are observed around 16, 24, 31, 38 and 49 (calendar) k-years. They are marked by increases in a few parameters (dust (%), Ti/Al, fibrous clay minerals, mean particle diameter). When compared to the glacial background, LLEs are identified as dustier events: their dust content increased by 10% to 25% and their coarse silt (>40 μm) particle content increased by ≈10%. The same pattern is also observed for the Younger Dryas event. We are aware that such increases could be also generated by dilution changes and thus, further flux evaluation will have to be made (using U-Th excess, for example). Mineralogical observations reveal that within these events, the terrigenous fraction is essentially made of clay, quartz and heavy minerals and that the dominant clay minerals are smectite (≈50%) and kaolinite (≈30%). Some other minor clay minerals reveal interesting variations; for example the amount of fibrous [palygorskite +sepiolite] clay minerals is 2 to 3 times more abundant during the LLEs. Finally, the isotopic composition (87Sr/86Sr, $\varepsilon_{Nd}(o)$) of the carbonate-free, fine (b40 μm) fraction, reveals homogenous results (Fig. 3 and Table 2). However, a slight difference is observed between the over- and underlying glacial dust and the LLE dust. The surrounding glacial dust displays Nd and Sr compositions, similar to the source values characterizing the western Sahara regions (area II on Figure. 3, i.e. western Senegal/Mauritania), while dust contained in the LLEs reveals more radiogenic Sr ratios similar to the source values characterizing more remote, inner African regions (area I on Figs. 1 and 3) (Grousset et al., 1998).

To a first approximation, these low-latitude events (LLE1–5) appear to be contemporaneous with the major ice sheet collapses that resulted in the HEs in the Northern Atlantic (Elliot et al., 2001). They stratigraphically correspond to (i) the IRD-rich HEs that we observed in core SU90- 11 (45°N), within the IRD belt (Jullien et al., 2006) (Figs. 1 and 2) and (ii) to some of the strong $\delta^{18}O$ minima recorded in the North-GRIP ice core (Fig. 2). Indeed, we could consider them as “Heinrich-like events”. However as they are not made of IRD, we more likely name them “low-latitude events”.

Discussion

Climatic changes control the importance and nature of the dust fraction. According to Rea (1994), the dust increase observed in the LLEs (≈10%) would require an increase in aridity over the nearby continent, compared with the aridity that characterized the Sahara desert during the last Glacial (Sarnthein, 1978). In parallel, the observed increase of the coarse (>40 μm) detrital fraction more likely reflects intensified winds (Rea, 1994). One

could expect that such wind intensification would enhance both deflation and transport processes, allowing then the uplift of the heaviest particles, such as heavy minerals. The clear increase of the Ti/Al ratios observed during the LLEs (Fig. 2) probably reflects the increased deflation by intensified winds of Ti-rich heavy minerals (e.g. ilmenite, sphene or rutile)—their density being twice that of quartz or feldspars.

Changes that affected the dust composition during LLEs could also reflect other forcing factors, such as changes in dust source regions. Studies describing modern transport of north African dust to the tropical Atlantic (Bergametti et al., 1989) reveal that three main regions were able to supply dust accumulated in core MD03-2705: (a) the Sahel region (Senegal, southern Mauritania, southern Mali); (b) the northern and western Sahara (northwestern Mauritania, Morocco, western Algeria); and (c) the southern and central Sahara (southeastern Mauritania, northern Mali, southern Algeria). The palygorskite abundance (≈10%) of such fibrous minerals observed within the LLEs allows us to rule out any Sahelian supply. Indeed, palygorskite can be considered as a tracer for mineral dust derived from the Sahara (Schütz and Sebert, 1987). Furthermore, the relative proportions of clay minerals (smectite >40%, kaolinite >15%, illite ≈10%, palygorskite ≈10%) are similar to those observed in present-day dust originating from southern Algeria and/or the eastern part of Ahaggar between Algeria and Libya (Coudé-Gaussen, 1988) (Fig. 1). This clay mineral assemblage cannot be found in the second potential source (western Mauritania, Morocco, western Algeria), where kaolinite and illite are much more abundant. Thus, solely based on clay mineral assemblages, the most probable dust source candidate should be located around southern Algeria (i.e. the Ahaggar region).

According to the Sr–Nd isotopic composition of the detrital, carbonate-free fine fraction of LLEs, it appears that this southern Algerian source should be enlarged to the SW Libyan region (area I on Figs. 1 and 3). During glacial intervals separating the LLEs, these remote source regions would have been less dominant, while dust inputs from nearby regions (Senegal, Southern Mauritania) would have increased slightly (region II on Fig. 1).

Palygorskite and sepiolite are usually abundant in lake sediments (Singer and Galan, 1984). Lakes developed across Sahara during humid periods, such as the early Holocene (deMenocal et al., 2000). During the last glacial – especially during the driest periods – these lakes could have dried up, in particular in the eastern areas such as Chad (Washington et al., 2006) and/or Ethiopia (H. Lamb, personal communication). The drying up of these lakes during the LLEs would have exposed these lacustrine minerals, allowing their deflation and

subsequent transport to the ocean. This interpretation is supported by the fact that during all the LLEs, the concentration of pollen (but also of lake-derived, freshwater diatoms (Barcena et al., personal communication, 2006), are increased by a factor of 2–4.

During periods between the LLEs, less abundant, finer dust inputs would be derived from the coastal regions (Senegal, Southern Mauritania) (Fig. 1). On the other hand, during the LLEs, intensified dryness and winds would also bring aerosols from more remote areas (e.g. southern Algeria/Libya, Chad), as suggested by the increase of lacustrine-derived components (e.g. fibrous clay minerals and freshwater diatoms). This is consistent with the simultaneous intensification (or enlargement?) of offshore-driven upwelling cells observed along the Mauritanian margin, as revealed by typical changes in planktic foraminifera assemblages (Eynaud et al., in preparation).

During present-day winters, aerosols falling over the studied area come from northern Mauritania, northern Mali and southwestern Algeria, as brief but intense pulses transported in the lower atmosphere (b1 km). The ITCZ is then located around 5°N, allowing the development of high pressure over NW Africa and generating NE continental trade winds. Similarly, we may hypothesize that during glacial periods, intensified dust supplies should be expected, as meteorological patterns were similar to the present-day winter conditions, with the ITCZ moving southwards. Furthermore, to transport heavier and bigger particles, winds have to be intensified by a reinforcement of the Azores high pressure zone. Thus, in order to produce low latitude dusty events, aridity might have increased at these latitudes, and both SAL and trade winds should have been intensified.

Interestingly, it must be pointed out that similar arid LLEs were also observed in other tropical regions. Although these studies were not conducted at a high resolution mode, this is the case off Cameroon (Adegbie et al., 2003), off Somalia (Ivanochko et al., 2005), in the eastern Mediterranean (Bartov et al., 2003) or off Venezuela (Peterson et al., 2000). Similarly, synchronous dusty events observed in the Greenland ice cores (Mayewski et al., 1994) were interpreted as remote records of increased aridity over China (Biscaye et al., 1997). All these simultaneous signals of aridity would suggest a global atmospheric reorganization, at least in the northern hemisphere. However, it is clear that this reorganization is more complex, as for example, opposite signals were observed in some restricted tropical regions such as northeastern Brazil, where LLEs are characterized by increased precipitation events (Arz et al., 1998).

Finally, when looking at the dust (%) record in core MD03- 2705 (Fig. 2), it seems that – except for LLE1 – the dust amount reached its maximum during the upper part of each LLE. Interestingly, pollen observed off northwestern Spain reveal similar late arid events during the late part of HEs (Naughton et al., 2007). Such a signal could be interpreted as a response to the northern HEs, which is indeed suggested by model simulations (Hewitt et al., submitted for publication). However, based solely on our data, it would be too risky to claim that there is a systematic lag, until we may obtain a really tight time constraint across these events and accumulation rate calculations, which is not the case yet. The slightly different pattern observed for LLE1 (Fig. 2) – the dust % start to decrease in the middle of the event – could be due to the sudden global post-glacial warming that took place at that time, modifying drastically the atmospheric circulation and possibly interrupting prematurely this aridity event in the tropics.

Conclusions

The origin of the North Atlantic Heinrich events is still a matter of debate, although the "internal forcing" hypothesis (McAyeal, 1993) would meet a large consensus. It has been suggested that an alternate scenario could be provided by considering the tropical ocean–atmosphere system as providing that triggering mechanism (Broecker, 2003). Our high resolution study of a marine record located at lower latitudes (off the Saharan region) would suggest that, at a first approximation, abrupt "dusty" events occurred simultaneously to the classic, high-latitude "icy" Heinrich events. A much higher resolution and stronger constraints on the age model would be required to identify leads or lags, if any. Interestingly, similar aridity events were also observed in other regions of the northern hemisphere, thus pointing to a global signal probably associated with intensified southward shifts of the ITCZ. However, as locally opposite responses (e.g. higher precipitation over Brazil) were also reported during these events, the atmospheric reorganization triggered by the Heinrich events was probably more complex and its understanding would require more work, such as modelling approaches.

Acknowledgements

IMAGES core MD03-2705 was recovered by the N/V Marion-Dufresne (IPEV). I. Billy, P. Brunet, G. Chabaud, D. Poirier provided invaluable technical assistance. AMS-14C ages were measured by Beta Analytic Inc. We thank E. Schefuβ, S. Weldeab and U. Röhl for access to

the Bremen XRF core scanner (and measurements), as well as their financial RCOM support by the German Science Foundation (DFG). We have benefited from the fruitful reviews of P.E. Biscaye, T. Corrège, D. Rea and W. Fletcher. Financial contribution from the INSU ECLIPSE programme is acknowledged. This is UMR 5805 EPOC contribution 1656.

References

Adegbie, A.T., Schneider, R.R., Rohl, U., Wefer, G., 2003. Glacial millennial scale fluctuations in central African precipitation recorded in terrigenous sediment supply and freshwater signals offshore Cameroon. Palaeogeography, Palaeoclimatology, Palaeoecology 197, 323–333.

Arz, H.W., Patzold, J., Wefer, G., 1998. Correlated millennial-scale changes in surface hydrography and terrigenous sediment yield inferred from last glacial marine deposits off Northeastern Brazil. Quaternary Research 50, 157–166.

Bard, E., 1988. Correction of AMS 14C ages measured on planktonic foraminifera: paleoceanographic implications. Paleoceanography 3, 635–645.

Bartov, Y., Goldstein, S.L., Stein, M., Enzel, Y., 2003. Catastrophic arid episodes in the Eastern Mediterranean linked with the North Atlantic Heinrich events. Geology 31, 439–442.

Bergametti, G., Gomes, L., Remoudaki, E., Desbois, M., Martin, D., Buat- Ménard, P., 1989. Present transport and deposition patterns of African dust to the north-western Mediterranean. In: Leinen, M., Sarnthein, M. (Eds.), Paleoclimatology and Paleometeorology: Modern and Past Patterns of Global Atmospheric Transport. Kluxer Academic, pp. 227–252.

Biscaye, P.E., Grousset, F.E., Revel, M., Van der Gaast, S., Zielinsky, G.A., Vaars, A., Kukla, G., 1997. Asian provenance of Last Glacial Maximum dust in the GISP-2 ice core, Summit, Greenland. Journal of Geophysical Research 102, 26765–26781.

Boyle, E.A., 1983. Chemical accumulation variations under the peru current during the past 130 kyr. Journal of Geophysical Research 88, 7667–7680.

Broccoli, A.J., Dahl, K.A., Stouffer, R.J., 2006. Response of the ITCZ to northern hemisphere cooling. Geophysical Research Letters 33, L01702, doi:10.1029/2005GL024546.

Broecker, W.S., 2003. Does the trigger for abrupt climate change reside in the ocean or in the atmosphere? Science 300, 1519–1522.

Cane, M., Clement, A.C., 1999. A role for the tropical Pacific coupled ocean– atmosphere system on Milankovitch and millennial timescales. Part II: global impacts. Mechanisms of global climate change at millennial time scales. In: Clark, P.U., Webb, R.S., Keigwin, L.D. (Eds.), Geophys. Monographs, vol. 112. AGU, Washington, pp. 373–383.

Coudé-Gaussen, G., 1988. Contribution à l'étude sédimentologique des poussières sahariennes et à leur identification dans les sédiments continentaux et marins. Bulletin de la Societe Geologique de France 6, 1063–1072.

deMenocal, P., Ortiz, J., Guilderson, T., Adkins, J., Sarnthein, M., Baker, L., Yarusinsky, M., 2000. Abrupt onset and termination of the African Humid Period: rapid climate responses to gradual insolation forcing. Quaternary Science Reviews 19, 347–361.

Elliot, M., Labeyrie, L., Dokken, T., Manthe, S., 2001. Coherent patterns of ice-rafted debris deposits in the Nordic regions during the last glacial (10–60 ka). Earth and Planetary Science Letters 194, 151–163.

Grousset, F.E., Parra, M., Bory, A., Martinez, P., Bertrand, P., Shimmield, G., Ellam, R.M., 1998. Saharan wind regimes traced by the Sr–Nd isotopic composition of subtropical Atlantic sediments: Last Glacial Maximum vs today. Quaternary Science Reviews 17, 395–409.

Heinrich, H., 1988. Origin and consequences of cyclic ice rafting in the Northeast Atlantic Ocean during the past 130,000 years. Quaternary Research 29, 142–152.

Holtzapffel, T., 1985. Les minéraux argileux: préparation, analyse diffractométrique et détermination. Société Géologique du nord, Villeneuve d'Ascq. 136 p.

Husar, R.B., Prospero, J.M., Stowe, L.L., 1997. Characterization of tropospheric aerosols over the oceans with the NOAA Advanced Very High Resolution Radiometer Optical Thickness Operational Product. Journal of Geophysical Research 102, 889–909.

Imbrie, J., Hays, J.D., Martinson, D.G., McIntyre, A., Mix, A.C., Morley, J.J., Pisias, N.G., Prell, W.L., Shackleton, N.J., 1984. The orbital theory of a Pleistocene climate: support from revised chronology of the marine $\delta^{18}O$ record. In: Berger, A., Imbrie, J., Hays, J., Kukla, G., Saltzman, B. (Eds.), Milankovitch and Climate, Riedel, D, Dordrecht, pp. 269–305.

Ivanochko, T.S., Ganeshram, R.S., Brummer, G.-J.A., Ganssen, G., Jung, S.J.A., Moreton, S.G., Kroon, D., 2005. Variations in tropical convection as an amplifier of global climate change at the millennial scale. Earth and Planetary Science Letters 235, 302–314.

Jansen, J.H.F., Van der Gaast, S.J., Koster, B., Vaars, A.J., 1998. CORTEX, a shipboard XRF-scanner for element analyses in split sediment cores. Marine Geology 151, 143–153.

Johnsen, S., Dahl-Jensen, D., Gundestrup, N., Steffensen, J.P., Clausen, H.B., Miller, H., Masson-Delmotte, V., Sveinbjörnsdottir, A.E., White, J., 2001. Oxygen isotope and palaeotemperature records from six Greenland ice-core stations: Camp Century, Dye-3, GRIP, GISP2, Renland and NorthGRIP. Journal of Quaternary Science 16, 299–307.

Jullien, E., Grousset, F.E., Hemming, S.R., Peck, V.L., Hall, I.R., Jeantet, C., Billy, I., 2006. Contrasting conditions preceding MIS3 and MIS2 Heinrich events. Global and Planetary Change 54, 225–238.

Kolla, V., Biscaye, P.E., Hanley, A.F., 1979. Distribution of quartz in late Quaternary Atlantic sediments in relation to climate. Quaternary Research 11, 261–277.

Martinson, D.G., Pisias, N.G., Hays, J.D., Imbrie, J., Moore, T.C., Shackleton, N.J., 1987. Age dating and the orbital theory of the Ice Ages: development of a high-resolution 0 to 300,000-year chronostratigraphy. Quaternary Research 27, 1–29.

Matthewson, A.P., Shimmield, G., Kroon, D., Fallick, A.E., 1995. A 300 kyr high resolution aridity record of the North African continent. Paleoceanography 10, 677–692.

Mayewski, P.A., Meeker, L.D., Whitlow, S., Twickler, M.S., Morrison, M.C., Bloomfield, P., Bond, G., Alley, R.B., Gow, A.J., Grootes, P.M., Meese, D., Ram, M., Taylor, K.C., Wumkes, W., 1994. Changes in atmospheric circulation and ocean ice cover over the North Atlantic during the last 41,000 years. Science 263, 1747–1751.

McAyeal, D.R., 1993. Binge/purge oscillations of the Laurentide ice sheet as a cause of the North Atlantic' Heinrich events. Paleoceanography 8, 775–784.

Mie, G., 1908. Beiträge zur optik trüber Medien, speziell kolloidaler Metallösungen. Annalen der Physik, pp. 377–752.

Moyes, J., Duplantier, J., Duprat, J., Faugeres, J.C., Pujol, C., Pujos-Lamy, A., Tastet, J.P., 1976. Etude stratigraphique et sédimentologique. Geochimie organique des sédiments marins profonds, Orgon II, Atlantique N. In: Brésil, E. (Ed.), C.N.R.S., Paris, pp. 105–156.

Naughton, F., Sanchez Goni, M.F., Desprat, S., Turon, J.L., Duprat, J., Malaize, B., Joli, C., Cortijo, E., Drago, T., Freitas, M.C., 2007. Present-day and past (last 25 000 years) marine pollen signal off western Iberia. Marine Micropaleontology 62, 91–114.

Peterson, L.C., Haug, G.H., Hughen, K.A., Röhl, U., 2000. Rapid changes in the hydrologic cycle of the tropical Atlantic during the last Glacial. Science 290, 1947–1951.

Rea, D.K., 1994. The paleoclimatic record provided by Eolian deposition in the deep sea: the geologic history of wind. Review of Geophysics 32, 159–195.

Ruddiman,W.F., 1977. Late Quaternary deposition of ice-rafted sand in the subpolar North Atlantic (lat. 40° to 65°). Geological Society of America Bulletin 88, 1813–1821.

Sarnthein, M., 1978. Sand deserts during glacial maximum and climatic optimum. Nature 272, 43–46.

Schütz, L., Sebert, M., 1987. Mineral aerosols and source identification. Journal of Aerosol Sciences 18, 1–10.

Singer, A., Galan, E., 1984. Palygorskite–sepiolite: occurrences, genesis and uses. Developments in Sedimentology. Elsevier, Amsterdam. 352 p.

Skinner, L.C., McCave, I.N., 2003. Analysis and modelling of gravity- and piston coring based on soil mechanics. Marine Geology 199, 181–204.

Stuiver, M., Reimer, P., Reimer, R.W. (2005). CALIB 5.0.

Washington, R., Todd, M.C., Lizcano, G., Tegen, I., Koren, I., Ginoux, P., Engelstaedter, S., Bristow, C., Zender, C.S., Goudie, A., Warren, A., Prospero, J.M., 2006. Links between topography, wind, deflation, lakes and dust: the case of the Bodélé Depression, Chad. Geophysical Research Letters 33 L09401,10.1029/2006GL025827.

Figure Captions

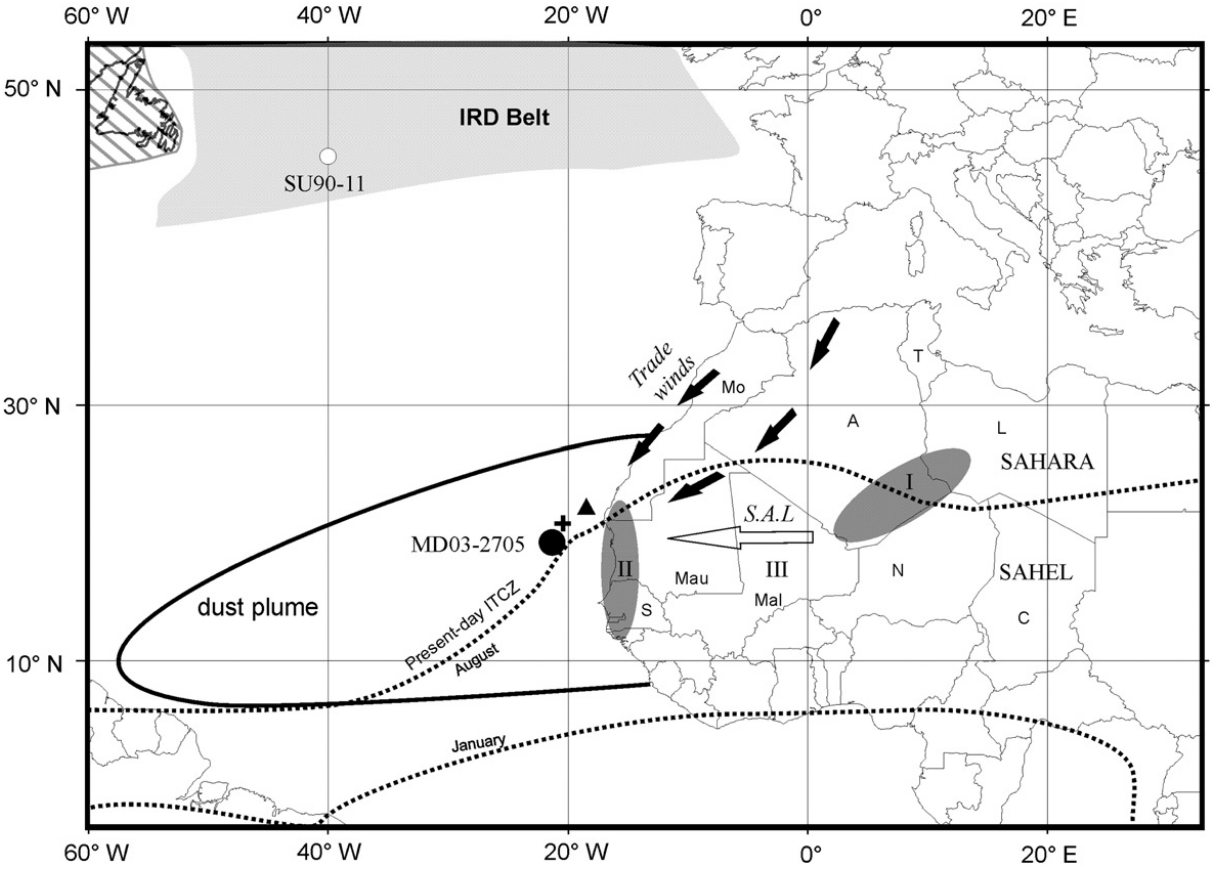

Figure 1. Location of cores MD03-2705 (closed circle), SU90-11 (open circle), CD53-30 (cross) and ODP-658C (closed triangle). The light-grey band represents the IRD belt (Ruddiman, 1977); the contoured, dashed area represents the southeastern tip of the Laurentide ice sheet. Over Africa, the remote Saharan dust source (#I) and the nearby dust source (Mauritania/Senegal) (#II) regions are highlighted with a grey pattern. Open arrows represent the high altitude Saharan Air Layer (SAL) and dark arrows represent the low altitude Trade Winds. Countries are distinguished by a letter: A (Algeria), C (Chad), L (Libya), Mo (Morocco), Mal (Mali), Mau (Mauritania), N (Niger), S (Senegal), T (Tunisia). Dotted lines represent the present-day location of ITCZ in Northern hemisphere summer and winter.

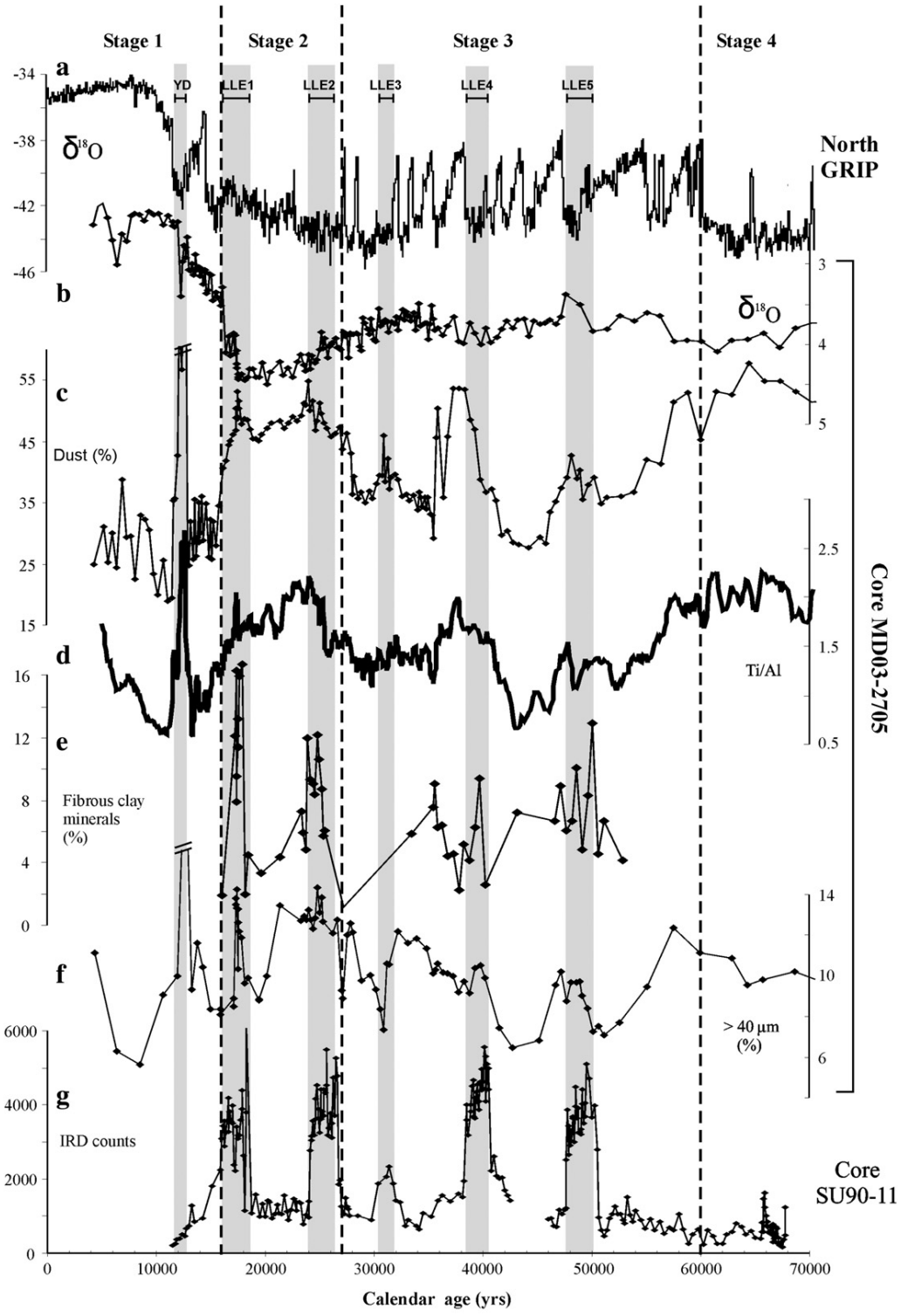

Figure 2. Temporal distribution of different parameters: (1) the $\delta^{18}O$ (a) North GRIP record (Johnsen et al., 2001); (2) in core MD03-2705, the $\delta^{18}O$ record of benthic foraminifera (b), the dust abundance (c), the Ti/Al ratio (d), the abundance of fibrous (palygorskite+sepiolite) clay minerals (e), the % of coarse (N40 µm) detrital particles (f); (3) in core SU90-11, the IRD record (Jullien et al., 2006). Vertical bands represent low-latitude events (LLEs) and Younger Dryas (YD) and vertical dotted lines are the isotopic stage boundaries.

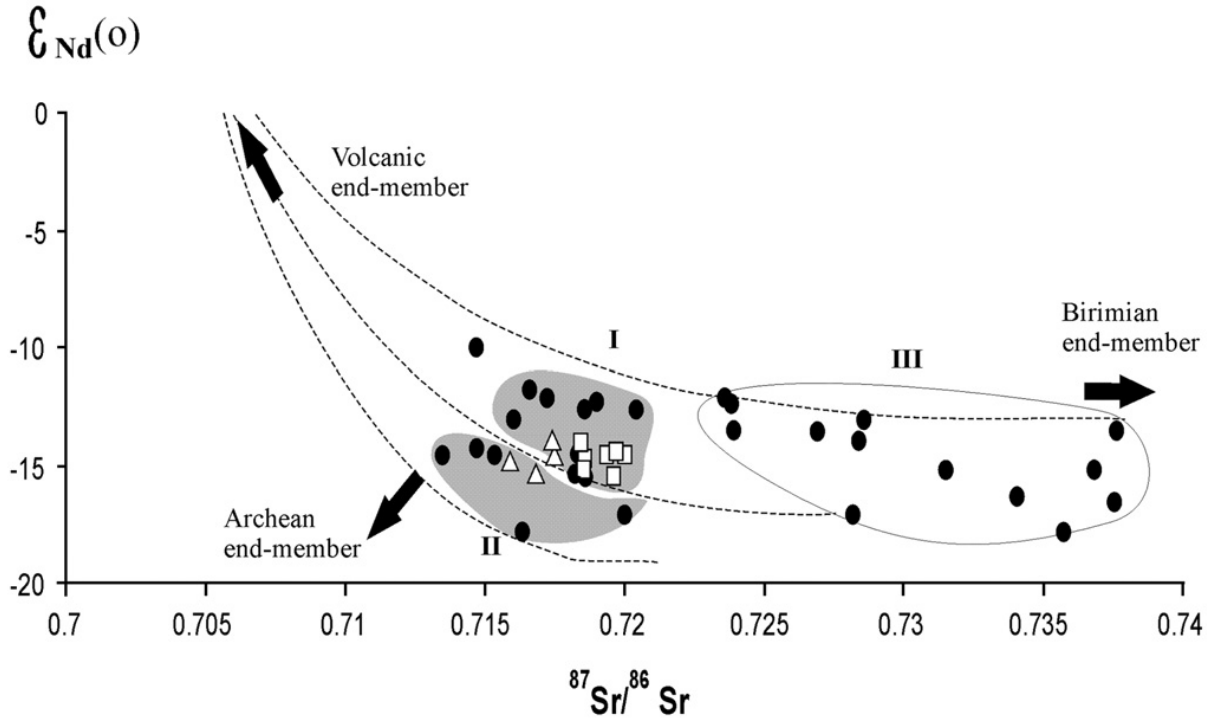

Figure 3. Isotopic composition (87Sr/86Sr-εNd(o)) of the carbonate-free, fine (<40 μm) fraction of (i) MD03-2705: LLEs (open squares); under-and overlying glacial sediments (open triangles); (ii) potential source areas (PSA) (closed circles from Grousset et al., 1998). Field I: remote PSA (Algeria and Libya); Field II: western PSA (Senegal, Southern Mauritania); Field III: southern Saharan/Sahelian PSA (Mali, Niger, Chad, etc.). PSAs, hyperbolic mixing curves and end-members are from Grousset et al., 1998.

Table 1

Age constraints used for building the MD03-2705 age model

Pointers	Depth (cm)	Corrected ^{14}C ages (ka)	Standard error	Calibration two sigma ranges* (cal yr BP)	Calendar ages (ka)	Source
AMS-^{14}C dating	3	4.38	40	5040–5300	5.19	1
Menardii	34	10		11370–11910	11.6	1
AMS-^{14}C dating	38	10.15	70	11690–12310	11.78	1
Tuned on ODP-658C	44	10.6		12670–12840	12.74	2
Inflata	85	12.46		14255–15063	14.72	1
AMS-^{14}C dating	94	13.01	80	15150–15880	15.49	1
AMS-^{14}C dating	112	14.38	40	16970–17800	17.31	1
Isotopes + inflata	126	14.95		18430–18680	18.5	1
AMS-^{14}C dating	142	16.74	60	19840–20160	19.98	1
AMS-^{14}C dating	160	19.8	100	23490–24160	23.84	1
AMS-^{14}C dating	176	21.21	120		24.99**	1
$\delta^{18}O$ benthic	198				27	4
$\delta^{13}C$ tuned on core SU90-08	294				35	3
AMS-^{14}C dating	302	30.77	350		35.82**	1
$\delta^{13}C$ tuned on core SU90-08	338				45	3
$\delta^{18}O$ benthic	400				60	4
$\delta^{18}O$ benthic	445				73	4
$\delta^{18}O$ benthic	495				85.55	4
$\delta^{18}O$ benthic	505				88.03	4
$\delta^{18}O$ benthic	695				124	4
$\delta^{18}O$ benthic	725				132.5	4

Sources: (1) this work; (2) deMenocal et al., 2000; (3) Vidal et al., 1998; (4) Martinson et al., 1987. Calendar ages, ∗ after Stuiver et al. (2005), ∗∗ after Bard (1988).

Table 2

Sr and Nd isotopic composition of fine (b40 μm), carbonate-free fraction of core MD03-2705

Depth (cm)	$^{87}Sr/^{86}Sr$	Error bar ($\times 10^6$)	$^{143}Nd/^{144}Nd$	Error bar ($\times 10^6$)	$\varepsilon_{Nd(0)}$	Events
49	0.719989	10	0.511886	9	−14.6	Younger Dryas
71	0.717373	12	0.511911	10	−14.1	Glacial background
122	0.718425	9	0.511918	11	−14	Low-latitude event 1
139	0.717431	8	0.511893	10	−14.5	Glacial background
166	0.719671	10	0.511897	8	−14.4	Low-latitude event 2
177	0.719357	9	0.511885	8	−14.6	Low-latitude event 2
223	0.716859	9	0.511853	8	−15.3	Glacial background
245	0.718461	10	0.511882	7	−14.7	Low-latitude event 3
311	0.719572	9	0.511845	9	−15.4	Low-latitude event 4
335	0.715849	9	0.511877	14	−14.8	Glacial background
355	0.718514	7	0.511859	6	−15.2	Low-latitude event 5

Nd isotope data are expressed as εNd(0).